Enhancing the Capacity of Large LEO Satellites with Internetworked Small Piggybacks for Low Latency Payload Data Transmission

V. Ramalakshmi
Department of ECE, KLEF, Vaddeswaram, Guntur, Andhra Pradesh, India | RO, Department of Space, UR Rao Satellite Centre, Bangalore, India
ramalakshmi66@gmail.com

Venkata Narayana Madhavareddy
Department of ECE, KLEF, Vaddeswaram, Guntur, Andhra Pradesh, India
mvn@kluniversity.in

Govardhani Immadi
Department of ECE, KLEF, Vaddeswaram, Guntur, Andhra Pradesh, India
govardhanee_ec@kluniversity.in (corresponding author)

V. V. Srinivasan
ISRO, Department of Space, UR Rao Satellite Centre, Bangalore, India
vvsrinivasan.jpn@gmail.com

Received: 10 April 2024 | Revised: 29 April 2024 | Accepted: 7 May 2024

Licensed under a CC-BY 4.0 license | Copyright (c) by the authors | *DOI: https://doi.org/10.48084/etasr.7449*

ABSTRACT

In most cases, the utilization of the costly payload onboard Low Earth Orbit (LEO) satellites is restricted by the limited throughput of the payload data downlink to the ground station during the visibility window. The usefulness of these data in critical applications reduces due to the large latency of the process. Different techniques involving efficient modulation schemes, increased power within the allowed level and frequency band, and capacity enhancement using close-by satellites have been studied and implemented with their relative merits and limitations in an attempt to reduce the latency of the data to the user. The present study proposes a constellation of low-cost data relay satellites placed in the same orbital plane along with the main satellite, increasing directly the effective visibility window. As a result, the utility of the main satellite is also increased by the same factor. A detailed analysis of the constellation and configuration of the relay satellites is presented in this paper.

Keywords-data transmission; internetworking; latency; LEO orbit;, satellite constellation; polar orbit

I. INTRODUCTION

Due to the proximity to the earth surface, the Low Earth Orbit (LEO) has always been a preferred platform for earth observation with very high-resolution imaging and scientific military or civilian applications. But these have resulted in increased volume of data gathered onboard. The visibility window to an earth station for a LEO satellite is about 10-12 min per orbit [1] and 3-4 orbits in a day. Hence, downloading large volumes of data using the available bandwidth [2] from the satellite has become a new challenge. In many occasions, the utilization of the satellite is governed by this capacity. Multiple studies have tried to address this challenge [3-13]. They can be broadly classified into the following categories: (i) increasing the capacity of the available channel, (ii) exploiting larger bandwidth available at higher frequency bands, (iii) using multiple ground stations at geographically diverse locations, and (iv) increasing the effective time of transmission deploying satellite constellations. The capacity of a channel is governed by Shannon's theorem [14] and cannot be increased beyond a limit considering the limitation of onboard power, mass, open channel propagation, safe limit of radiation on ground, etc. Employing power and spectrum modulation [15-16], a system with 800 Mbps capacity was implemented in [17] covering the allocated X-band spectrum of 8-8.4 GHz. Orthogonal circular polarized link was put into service for frequency reuse [18, 19]. Considering all these, the highest data rate known so far is about 960 Mbps, which can transmit about

345 GB of data for a nominal contact time of 6 min for a nominal orbit height of 500 km and 10º elevation for start and stop of transmission. Migrating to a higher frequency band like the Ka- band is also another approach [20-27]. Data transmission in the Ka-band has several advantages, such as RF links supporting higher bit rates due to the availability of the 1.5 GHz allocated bandwidth, advantage derived from multi-beam satellites, user terminals with smaller antennas, etc. [22, 28]. Also, higher data rates can be achieved in this band using higher modulation techniques and frequency reuse techniques. Large rain attenuation at the Ka-band is a factor to be dealt with, specifically for tropical countries like India [20, 21]. Although a few space agencies have employed it, it is not a popular system yet considering the compatibility with the existing infrastructure [20, 21]. Placing additional ground stations at geographically diverse locations is another option. The international collaboration at the Antarctica is an example of that [29]. All the polar satellites pass over the polar region during every orbit. But, this can be exploited completely in multi-mission scenarios and constrained environment and there is the issue of the delay of relaying the received data to the processing centers. Another approach is to uplink the data to a geostationary (GEO) satellite which is visible to the ground station continuously [30, 31]. This scheme is quite regularly used by NASA for supporting the International Space Station (ISS) [32].

II. CONFIGURATION OF THE CONSTELLATION

Typical constellation configurations with one main satellite supported by four relay satellites is shown in Figure 1. The main satellite may be carrying very sub-meter resolution imaging payload or RADAR imaging payloads generating large data. A typical satellite imaging with a resolution of 6.4 m × 15 m and swath area of 240 km for about 10 min generates about 2.6 Tb of data and with the technological advance, the data volume is expected to go higher. As the onboard storage is limited, or in case of urgent requirement, the data have to be transmitted to the ground.

A typical satellite to ground link as evidenced in Table I, at 26.25 GHz with 1500 MHz bandwidth, can transmit 2.16 Tb using onboard EIRP of 33.3 dBW and ground station G/T of 36.5 dB/K, in one orbit. The balance of 4.84 Tb has to be transmitted to the ground station by Terminal Satellites (TSs). This dictates the capacity and the number of TSs required. All the terminal satellites may follow the main satellite as in Figure 1(a) giving some time advantage in case of real time simultaneous imaging and transmitting. But the distance from the main satellite increases with each additional satellite, and additional power for inter-satellite link is needed. A symmetric distribution with few satellites preceding the main satellite as in Figure 1(b) helps reducing the separation between them and is very well suited for non-real time operations. Different scenarios considering these cases are analyzed in [34].

The satellite visibility to ground is limited and is based on various orbital parameters like orbital height, inclination, and angle of true anomaly [1]. This scheme is planned to enhance the duration of the visibility window by making use of additional TSs which, in cooperation with the Master Satellite (MS) help to synthesize a larger visibility window to the ground station and thus enable data transfer of a larger volume of data with zero or minimum latency.

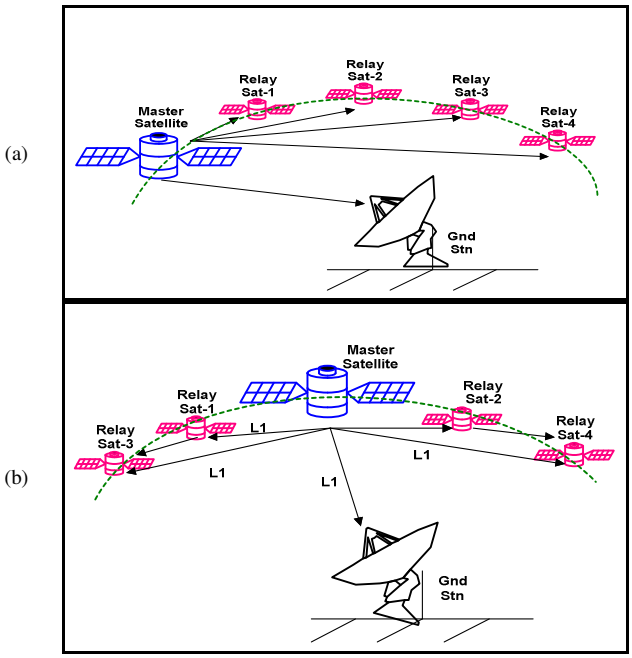

Fig. 1. Typical configuration of the constellation involving 4 relay satellites: (a) All satellites follow the main satellite, (b) relay satellites are distributed in fore and aft configuration

The imaging takes place in the MS only and data are transferred to the TSs through RF links, for subsequent transmission to the ground station. The RF link details from satellite to the ground station and intersatellite links for 30° (scenario-1) and 15° (scenario-2) true anomaly are provided in Table I. The link parameters for the 3 cases are not identical as the specification of each link is optimized for maximizing the throughput.

TABLE I. DIFFERENT RF LINK PARAMETERS

Parameter	Satellite to ground station	ISL scenario-1	ISL scenario-2
Frequency (MHz)	27000	27000	27000
Orbit height (km)	600	600	600
Range (km)	1932.4	3600	1803.9
Path loss (dB)	186.8	192.2	186.2
Data rate (Mbps)	2250.0	500.0	2250.0
Antenna diameter (m)	0.035	0.035	0.035
Ant gain	36	36	36
Tx. power (W)	2	4	4
Onboard loss (dB)	4	5.7	5.7
EIRP (dBW)	33.3	37.3	37.3
Losses (pointing, polarization, atmospheric, etc.)	4.6 dB	1 dB	1 dB
G/T (dB/K)	36.5	23	23
Eb/N0 available(dB)	16.0	8.7	8.2
Required Eb/N0(dB)	14.0	10.8	10.8
Implementation margin	2.5 dB	2.5 dB	2.5 dB
Coding gain	6 dB	6.0 dB	6.0 dB
Link margin	3 dB	1.4 dB	0.9 dB

The calculations for the satellite to the ground station link considers the scenario where two independent chains, in two orthogonal polarizations and each supporting a data rate of 2250 Mbps using 8PSK modulation, are considered to support the throughput of 4.5 Gbps. It is observed that for the LEO orbit under consideration, a link margin of 3 dB is achieved. ISLs in LEO orbits discussed for applications like extending coverage in personal communications [26], have expressed increased complexity in the ISL RF link. This aspect is addressed in this study by utilizing, similar technology for the ISL as that developed for the satellite-to-ground link. The range of the ISL increases with the angle of true anomaly. Limitations created by the onboard scenario constrain the onboard receive system G/T to much lower values in comparison with the ground system. Regarding the EIRP and G/T of the onboard systems, QPSK modulation and reduced data rates are considered for the ISL to maintain a margin comparable to the communication link with the ground station. The methodology for computation of data rates is discussed below.

III. TOPOLOGY OPTIMIZATION FOR AN INTERNETWORKING SATELLITE

As explained earlier, 7 Tb of image data is to be transmitted to the ground and the master satellite can transmit 2.16 Tb in one pass over a ground station. The balance 4.84 Tb has to be transmitted to the ground station by the three TSs. The load on each terminal satellite is 1.61 Tb. In order to arrive at the topology for internetworking, two limiting conditions as shown in Table II are considered. The Satellite Tool Kit simulator STK 12 Professional has been used to simulate and study the orbital dynamics of the satellites.

TABLE II. ORBITAL PARAMETERS FOR INTERNETWORKING

Orbital parameter	Scenario-1	Scenario-2
Orbit height	600 km	600 km
True anomaly	30°	15°
Range to ground station	1932.4 km	1932.4 km
Inter-satellite range	3600 km	1803.9 km

- Scenario-1: Network optimized for minimal overlap in the visibility of satellites.
- Scenario-2: Network optimized for maximum throughput.

Time available to transfer data from the MS to the TSs is more in Scenario-1 than in Scenario-2. Also, the range between the satellites is more in Scenario-1 (3600 km) than in Scenario-2 (1803.9 km). For these ranges the maximum data rates that can be supported on each RF chain with positive link margin are 500 Mbps and 2250 Mbps, respectively. But as sufficient bandwidth is available, it is possible to configure multi-beam transmission to meet higher data rate requirements.

A. *Scenario-1: No overlap in Satellite Visibility*

STK Scenario settings:

- Orbit: Polar Sun synchronous
- Altitude: 600 km
- Ground station Hyderabad (Hyd), India - minimum elevation angle: 10°
- Number of satellites: 4
- True anomaly separation between satellites: 30°

Figure 2 represents a condition where there is no satellite-to-ground visibility overlap, as the true anomaly angle between satellites is 30°. But the inter-satellite range is about 3600 km as compared to 1932.4 km to the ground station. The path loss is higher by 5.8 dB.

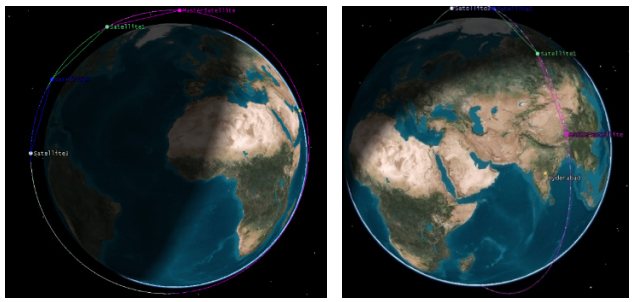

Fig. 2. Scenario-1 satellite positions.

Hence, data transfer between satellites can take place only at a reduced rate in order to maintain the RF link. Therefore, for seamless data transmission to ground, the payload data should be available (or imaging session should almost conclude) much ahead of Acquisition of Signal (AoS) of the MS to ground station as depicted in Figure 3. Best case condition is: 7 Tb of payload data has been imaged and 4.84 Tb of data that cannot be transmitted to ground directly by the MS are transferred to the TSs by the AoS time of MS. If imaging and data dumping have to happen without time gap, then synthesizing a larger window will be handled with more powerful data links and higher RF powers. Table III lists the AoS and Loss of Signal (LoS) of the MS and the 3 TSs. It should be noted from Table III that data transmission can happen between 6:45:54 and 07:17:56, i.e. in 32 min after imaging is completed. Also, the present study has succeeded in synthesizing a larger visibility window of 32.72 min as compared to the 7.798 min that would have been available with a single satellite.

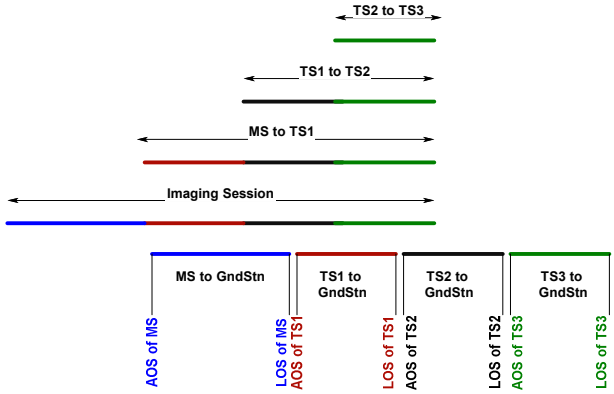

Fig. 3. Scenario-1 timeline for imaging and data transfer.

TABLE III. SCENARIO-1 SATELLITE VISIBILITY WITHOUT OVERLAP

	AoS Date and time	**LoS Date and time**	**Visibility time (min)**
Hyd-To-MS	14Dec2020 06:45:54.567	14Dec2020 06:53:42.475	7.798
Hyd-To-TS1	14Dec2020 06:53:42.902	14Dec2020 07:01:51.339	8.14
Hyd-To-TS2	14Dec2020 07:01:34.999	14Dec2020 07:09:55.904	8.348
Hyd-To-TS4	14Dec2020 07:09:30.495	14Dec2020 07:17:56.512	8.434
Synthesized Window			32.72

The flowchart in Figure 4 displays the methodology to be followed to identify satellite paths and to transfer data to them for dumping to the ground station in Scenario-1.

Fig. 4. Scenario-1 flowchart for satellite identification and data transfer.

The MS receives the ephemeris data of all the satellites (MS, TS1, TS2, and TS3) in orbit and calculates their AoS and LoS for the ground station. From the AoS and LoS and also the data rate supported by each satellite, it calculates the quantum of data each satellite can transmit to the ground as DMS, DTS1, DTS2, and DTS3. The payload data are suitably segmented as shown in Figure 5.

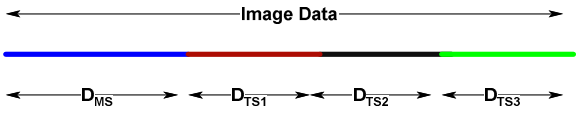

Fig. 5. Scenario-1 data segmentation.

The MD retains DMS data and transfers DTS1, DTS2, and DTS3 data to TS1, which retains DTS1 and transfers DTS2 and DTS3 data to TS2, which in-turn retains DTS2 and transfers DTS3 data to TS3. Based on the calculated AoS and LoS values, each satellite transmits its designated data to the ground station, thus achieving near real time transmission. Also, data transfer in the inter-satellite link is independent of the data transfer from satellite to the ground. The satellite systems should be capable of executing the two tasks independently, provided the criteria stated in the flowchart in Figure 4 are met.

B. Unit Scenario-2: Overlap in Satellite Visibility

STK Scenario settings:

- Orbit: Polar Sun synchronous
- Altitude: 600 km
- Ground station (Hyderabad) - minimum elevation angle: 10°
- Number of satellites: 4
- True anomaly separation between satellites: 15°
- Inter satellite range to nearest satellite at fore end/ aft end: 1821 km

Figure 6 represents the satellite positions in orbit when the true anomaly separation between them is reduced to 15° and the inter-satellite and satellites to ground station ranges are similar. Hence, the data transfer between satellites can be done at a similar rate as to ground station. As noticed in Figure 7, there are at least 2 satellites simultaneously transmitting data to the ground.

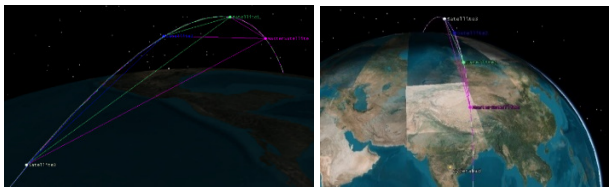

Fig. 6. Scenario-2 satellite positions.

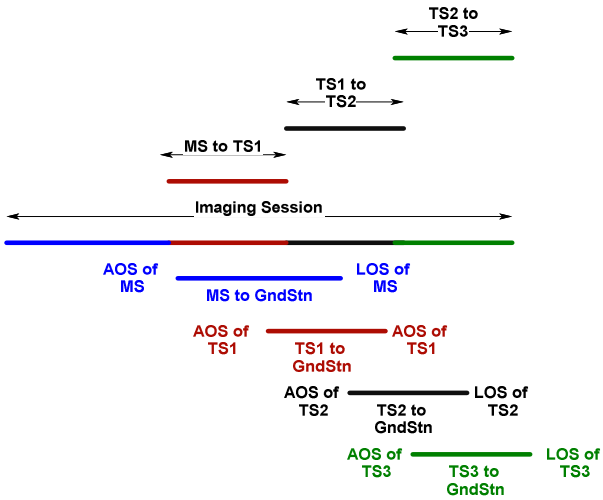

Fig. 7. Scenario-2 timeline for imaging and data transfer.

The benefit of this option is that data are transmitted to the ground in almost real time. The total time taken is also less (06:57:38 to 07:17:56, i.e 20 min). Here also a larger visibility window of 33.448 min has been synthesized as compared to the 8.26 min available with a single satellite. In these 20 min, 33.448 min visibility is achieved. Table IV lists the AoS and LoS of the MS and the 3 TSs. It can be seen that there is an overlap in satellite visibility to the ground. As the angle of true anomaly is smaller, the range between the satellites is smaller. Therefore, the RF link will support a faster rate of data transfer as compared to Scenario-1. As the time gap between the AoS of consecutive satellites is less, faster rate of data transfer is mandatory too.

TABLE IV. SCENARIO-2 SATELLITE VISIBILITY WITH OVERLAP

	AoS Date and time	**LoS Date and Time**	**Visibility time (min)**
Hyd-To-MS	14Dec2020 06:57:38.450	14Dec2020 07:05:54.07	8.26
Hyd-To-TS1	14Dec2020 07:01:34.939	14Dec2020 07:09:55.843	8.348
Hyd-To-TS2	14Dec2020 07:05:32.28	14Dec2020 07:13:56.629	8.406
Hyd-To-TS3	14Dec2020 07:09:30.495	14Dec2020 07:17:56.512	8.434
Synthesized Window			33.448

The flowchart in Figure 8 indicates the methodology to be followed to identify satellite paths and to transfer data to them for dumping to the ground station in Scenario-2. In this scheme too, based on the ephemeris data, the AoS, LoS and visibility time of all the satellites are computed and the data to be transmitted are suitably segmented as in Figure 5. The difference from Scenario-1 lies in the inter-satellite data transfer. As displayed in Figure 8, the MS retains the DMS data and transfers DTS1, DTS2, and DTS3 data to TS1, TS2, and TS3, respectively. When satellite AoS occurs, they start transmitting the data to the ground station. Here too, as in Scenario-1, data transfer in the inter-satellite link is independent of the data transfer from the satellite to the ground and the satellite systems should be capable of executing the two tasks independently, provided the criteria stated in the flowchart in Figure 8 are met.

This scheme puts two constraints: (1) Data should be available before AoS of the satellite. (2) As two satellites will be simultaneously transmitting to the ground station, the ground infrastructure should support the data reception. Also, as multiple satellites are visible to the MS, multi-beam transmission on the MS can be planned in order to simultaneously transfer data to multiple satellites. Multi beam phased array antennas using frequency reuse techniques have been proven in S, X, K/Ka bands [9-13], both in transmit and receive modes. Designs exist for the development of miniaturized phased array antennas in the Ka-band. TS1 retains DTS1 data and transfers DTS2 and DTS3 data to TS2, which in-turn retains DTS2 data and transfers DTS3 data to TS3. Based on the calculated AoS and LoS values, each satellite transmits its designated data to the ground station, thus achieving near real time transmission.

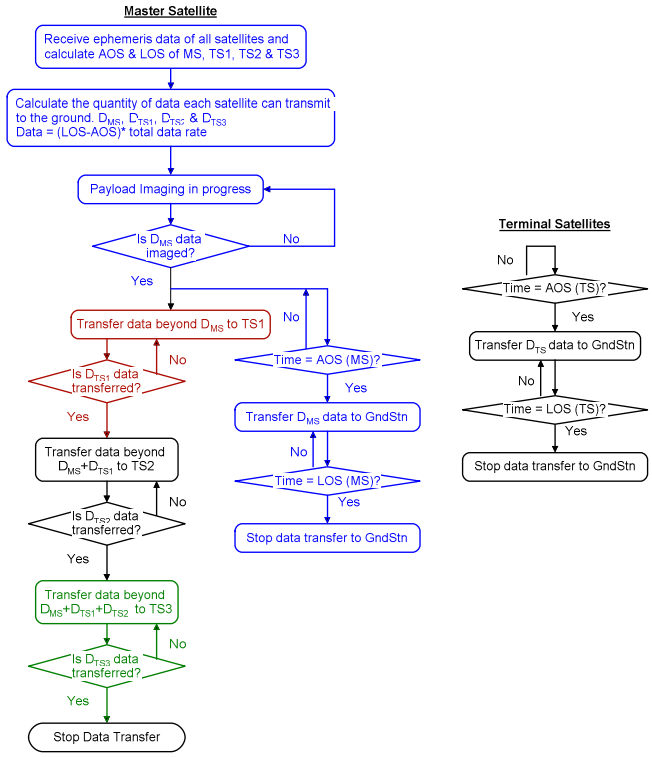

Fig. 8. Flowchart for satellite identification and data transfer.

IV. DISCUSSION

Two scenarios are discussed above. Scenario-1 with no overlap in the satellite visibility to the ground and hence constraints in the imaging session and larger latency. Scenario-2 does not impose constraint on the imaging session and image data volume. Also, data dump is almost real time.

In Scenario-1, the time taken to transmit data to the ground station increased to 32 min, in contrast to the ~8 min available from a single satellite. In Scenario-2 there is an overlap in satellite(s)-to-ground station visibility. The cumulative satellite(s) visibility to the ground is about 33 min, and due to the overlap of visibility to ground station it is possible to transmit the same amount of data to earth station in just 20 min. Two ground station terminals should be installed to receive data simultaneously owing to satellite visibility overlap in Scenario-2. Once the data are downloaded to the ground almost in real-time, the satellite is again ready to operate its payload. This effectively increases the usefulness of the satellite significantly. In both cases, where inter-satellite data transfer is proposed, it should be borne in mind that in addition to Ka-band transmission, Ka-band receiver supporting similarly high data rates is also to be conceived. A 50 Mbps data rate receiver in the Ka-band using COTS components has been documented [35]. State-of-the-art technologies can be utilized for higher data rates.

V. CONCLUSION

A constellation of satellites, a network of multiple satellites working together, offers a wide array of applications across various fields. Global Navigation Satellite Systems provide

accurate positioning, navigation, and timing services. Earth Observation Satellites in constellation can capture high-resolution images of Earth's surface for applications like environmental monitoring, disaster response, urban planning, agriculture, forestry management, and resource exploration. Communication Satellite constellations are used for global broadband internet coverage, especially in remote or rural areas where terrestrial infrastructure is insufficient, and facilitate long-distance communication, including voice, video, and data transmission for telecommunication services, television broadcasting, and maritime and aviation communication. Weather Forecasting Satellite constellations equipped with weather monitoring instruments provide data for weather forecasting, climate research, and monitoring natural disasters like hurricanes, typhoons, and wildfires. Military and civilian agencies use satellite constellations for surveillance, reconnaissance, border security, and monitoring of critical infrastructure.

Other applications include Search and Rescue, Precision Agriculture, Mapping, and Cartography. While these are just a few examples, of the applications of satellite constellations, the near-real time transmission of high volume data in the order of 7 Tb has not been explored yet. Also the configurations suggested in this paper are just a beginning and can easily be expanded for multiples of 7 Tb of data. The aim of this research is mainly to study the feasibility of high volume near real time data transmission and subsequently to develop a communication algorithm between satellites to achieve this goal.

REFERENCES

[1] M. H. Kaplan, *Modern spacecraft dynamics and control*. New York, NY, USA: John Wiley and Sons, 1976.

[2] *SA.1026-3 - Interference criteria for space-to-earth data transmission systems operating in the earth exploration-satellite and meteorological-satellite services using satellites in low-earth orbit*. ITU.

[3] X. Jia, T. Lv, F. He, and H. Huang, "Collaborative Data Downloading by Using Inter-Satellite Links in LEO Satellite Networks," *IEEE Transactions on Wireless Communications*, vol. 16, no. 3, pp. 1523–1532, Mar. 2017, https://doi.org/10.1109/TWC.2017.2647805.

[4] M. Zhang and W. Zhou, "Energy-Efficient Collaborative Data Downloading by Using Inter-Satellite Offloading," in *IEEE Global Communications Conference*, Waikoloa, HI, USA, Dec. 2019, pp. 1–6, https://doi.org/10.1109/GLOBECOM38437.2019.9013462.

[5] N. Yarr and M. Ceriotti, "Optimization of Intersatellite Routing for Real-Time Data Download," *IEEE Transactions on Aerospace and Electronic Systems*, vol. 54, no. 5, pp. 2356–2369, Oct. 2018, https://doi.org/10.1109/TAES.2018.2815880.

[6] R. Wang, A. Talgat, M. A. Kishk, and M.-S. Alouini, "Conditional Contact Angle Distribution in LEO Satellite-Relayed Transmission," *IEEE Communications Letters*, vol. 26, no. 11, pp. 2735–2739, Nov. 2022, https://doi.org/10.1109/LCOMM.2022.3196152.

[7] J. Zhang, S. Zhu, H. Bai, and C. Li, "Optimization Strategy to Solve Transmission Interruption Caused by Satellite-Ground Link Switching," *IEEE Access*, vol. 8, pp. 32975–32988, 2020, https://doi.org/10.1109/ACCESS.2020.2973698.

[8] F. Wang, D. Jiang, Z. Wang, Z. Lv, and S. Mumtaz, "Fuzzy-CNN Based Multi-Task Routing for Integrated Satellite-Terrestrial Networks," *IEEE Transactions on Vehicular Technology*, vol. 71, no. 2, pp. 1913–1926, Feb. 2022, https://doi.org/10.1109/TVT.2021.3131975.

[9] F. Cuervo, J. Ebert, M. Schmidt, and P.-D. Arapoglou, "Q-Band LEO Earth Observation Data Downlink: Radiowave Propagation and System Performance," *IEEE Access*, vol. 9, pp. 165611–165617, 2021, https://doi.org/10.1109/ACCESS.2021.3133390.

[10] T. De Cola and M. Marchese, "Performance analysis of data transfer protocols over space communications," *IEEE Transactions on Aerospace and Electronic Systems*, vol. 41, no. 4, pp. 1200–1223, Oct. 2005, https://doi.org/10.1109/TAES.2005.1561883.

[11] R. Radhakrishnan, W. W. Edmonson, F. Afghah, R. M. Rodriguez-Osorio, F. Pinto, and S. C. Burleigh, "Survey of Inter-Satellite Communication for Small Satellite Systems: Physical Layer to Network Layer View," *IEEE Communications Surveys & Tutorials*, vol. 18, no. 4, pp. 2442–2473, 2016, https://doi.org/10.1109/COMST.2016.2564990.

[12] Y. Su, Y. Liu, Y. Zhou, J. Yuan, H. Cao, and J. Shi, "Broadband LEO Satellite Communications: Architectures and Key Technologies," *IEEE Wireless Communications*, vol. 26, no. 2, pp. 55–61, Apr. 2019, https://doi.org/10.1109/MWC.2019.1800299.

[13] R. Deng, B. Di, and L. Song, "Ultra-Dense LEO Satellite Based Formation Flying," *IEEE Transactions on Communications*, vol. 69, no. 5, pp. 3091–3105, May 2021, https://doi.org/10.1109/TCOMM.2021.3058370.

[14] B. Sklar, *Digital Communications Fundamentals and Applications 2nd Edition*, 2nd Edition. Hoboken, NJ, USA: Prentice Hall, 2001.

[15] A. Kubra, R. K. Karunavati, P. Das, Y. Prasad, and W. R. Gautam, "Design of A Reconfigurable Digital Modulator For High Bit Rate Data Transmission," in *IEEE International Conference on Electronics, Computing and Communication Technologies*, Bangalore, India, Jul. 2020, pp. 1–6, https://doi.org/10.1109/CONECCT50063.2020.9198620.

[16] Md. G. Sadeque, "Bit Error Rate (BER) Comparison of AWGN Channels for Different Type's Digital Modulation Using MATLAB Simulink," *American Scientific Research Journal for Engineering, Technology, and Sciences*, vol. 13, no. 1, pp. 61–71, Jun. 2015.

[17] A. Gunderson and T. Tao, "X-band telecommunications design for large data volume earth observing missions," in *IEEE Aerospace Conference*, Big Sky, MT, USA, Mar. 2010, pp. 1–18, https://doi.org/10.1109/AERO.2010.5446957.

[18] V. V. Srinivasan, C. Kumar, B. P. Kumar, V. K. Lakshmeesha, and S. Pal, "Design considerations for dual circularly polarized spherical phased array antenna at X-band for spacecraft data transmission," in *IEEE Applied Electromagnetics Conference*, Kolkata, India, Dec. 2011, pp. 1–4, https://doi.org/10.1109/AEMC.2011.6256904.

[19] C. Kumar, B. P. Kumar, V. S. Kumar, and V. V. Srinivasan, "Dual Circularly Polarized Spherical Phased-Array Antenna for Spacecraft Application," *IEEE Transactions on Antennas and Propagation*, vol. 61, no. 2, pp. 598–605, Feb. 2013, https://doi.org/10.1109/TAP.2012.2220328.

[20] J. Rosello, A. Martellucci, R. Acosta, J. Nessel, L. E. Braten, and C. Riva, "26-GHz data downlink for LEO satellites," in *6th European Conference on Antennas and Propagation*, Prague, Czech Republic, Mar. 2012, pp. 111–115, https://doi.org/10.1109/EuCAP.2012.6206717.

[21] M. Jefferies, K. Maynard, P. Garner, J. Mayock, and P. Deshpande, "26-GHz data downlink and RF beacon for LEO in orbit demonstrator satellite," in *International Workshop on Tracking, Telemetry and Command Systems for Space Applications*, Noordwijk, Netherlands, Sep. 2016, pp. 1–5.

[22] D. Venugopal, C. Muthugadahalli, K. S. Mohanavelu, and K. Narayanan, "Ka band satellite communication systems-Applications and configurations," in *International Astronautical Congress*, Jerusalem, Israel, Oct. 2015, pp. 1–5.

[23] G. Busuttil-Reynaud and L. J. Elliott, "A multi service mobile satellite communications system operating at Ka-band," in *IEE Colloquium on Future of Ka Band for Satellite Communications*, London, UK, Nov. 1993, pp. 8/1-8/7.

[24] J. Wakeling, "System design constraints for a Ka-band satellite personal communications system," in *IEE Colloquium on Future of Ka Band for Satellite Communications*, London, UK, Nov. 1993, pp. 2/1-2/6.

[25] R. Acton, "Taking satellite and terrestrial broadband further," in *IET Seminar on Beyond Ka-Band: Meeting the Communication Bandwidth Requirements of the Future*, London, UK, Nov. 2011, pp. 1–24, https://doi.org/10.1049/ic.2011.0220.

[26] P. Jung, P. Fraise, M. Mazzella, E. Melet, and D. Rouffet, "Inter-satellite links for personal communications low Earth orbit satellite systems," in *3rd European Conference on Satellite Communications*, Manchester, UK, Nov. 1993, pp. 246–250.

[27] F. Alimenti *et al.*, "K/Ka-Band Very High Data-Rate Receivers: A Viable Solution for Future Moon Exploration Missions," *Electronics*, vol. 8, no. 3, Mar. 2019, Art. no. 349, https://doi.org/10.3390/electronics8030349.

[28] B. P. Kumar, P. Ratnakar Deokule, C. Kumar, C. Sriharsha, and V. S. Kumar, "Design of a Compact Steerable Reflector Antenna at Ka-Band in Axially Dispaced Ellipse Geometry," in *Indian Conference on Antennas and Propogation*, Ahmedabad, India, Dec. 2019, pp. 1–3, https://doi.org/10.1109/InCAP47789.2019.9134686.

[29] D. L. Brandel, W. A. Watson, and A. Weinberg, "NASA's advanced tracking and data relay satellite system for the years 2000 and beyond," *Proceedings of the IEEE*, vol. 78, no. 7, pp. 1141–1151, Jul. 1990, https://doi.org/10.1109/5.56928.

[30] G. Toso, M. Sabbadini, and G. Crone, "Characterisation of the RF channel between the ATV-ISS composite and TDRSS: modelling and modelling needs," in *IEEE Antennas and Propagation Society International Symposium. 2001 Digest. Held in conjunction with: USNC/URSI National Radio Science Meeting (Cat. No.01CH37229)*, Boston, MA, USA, Jul. 2001, vol. 4, pp. 750–753 vol.4, https://doi.org/10.1109/APS.2001.959574.

[31] A. C. Clarke, "Extra-Terrestrial Relays: Can Rocket Stations Give World-wide Radio Coverage?," in *Wireless World*, London, UK: Highbury Communications, 1945, pp. 305–308.

[32] A. U. Zaman, L. Manholm, and A. Derneryd, "Dual beam phased array antenna with wide scan angle for repeater applications," in *International Conference on Electrical and Computer Engineering*, Dhaka, Bangladesh, Dec. 2008, pp. 755–759, https://doi.org/10.1109/ICECE.2008.4769310.

[33] N. K. Majji, V. N. Madhavareddy, G. Immadi, N. Ambati, and S. M. Aovuthu, "Analysis of a Compact Electrically Small Antenna with SRR for RFID Applications," *Engineering, Technology & Applied Science Research*, vol. 14, no. 1, pp. 12457–12463, Feb. 2024, https://doi.org/10.48084/etasr.6418.

[34] N. K. Majji, V. N. Madhavareddy, G. Immadi, and N. Ambati, "A Low-Profile Electrically Small Serrated Rectangular Patch Antenna for RFID Applications," *Engineering, Technology & Applied Science Research*, vol. 14, no. 2, pp. 13611–13616, Apr. 2024, https://doi.org/10.48084/etasr.6989.

[35] N. Ambati, G. Immadi, M. V. Narayana, K. R. Bareddy, M. S. Prapurna, and J. Yanapu, "Parametric Analysis of the Defected Ground Structure-Based Hairpin Band Pass Filter for VSAT System on Chip Applications," *Engineering, Technology & Applied Science Research*, vol. 11, no. 6, pp. 7892–7896, Dec. 2021, https://doi.org/10.48084/etasr.4495.